

## SECONDARY DROPLET FORMATION DURING BINARY SUSPENSION DROPLET COLLISIONS

O. Kurt, U. Fritsching and G. Schulte

Department of Chemical Engineering, University of Bremen, Badgasteiner Strasse 3,  
28359 Bremen, Germany  
Phone: ++49 421 218 4778, Fax: ++49 421 218 7505  
Email: kurt@iwt.uni-bremen.de

### ABSTRACT

The outcome of collision dynamics of suspension drops (process fluids) is an interesting and challenging problem in industrial spray applications as e.g. spray drying. As a result of the liquid fragmentation process as well as a result of a binary droplet collision in the spray, fine droplets may be formed at the very low end of the overall droplet size distribution in the spray. The fine particles (dust) during spray drying are considered to be a difficult process to control. One of the main causes is the complex interaction of suspension droplets in the hot air flow and the collision of droplets. An experimental study of binary collisions of suspension droplets in off center collisions (impact parameter of  $B > 0$ ) is discussed. The aim is to study the collision phenomena and derive dominant physical mechanisms of binary droplet collision of suspensions. Two suspension droplet streams of equal size have been generated by means of piezoelectric droplet generators. The drop velocities of the two streams of suspension drops have been varied systematically to change the Weber number of the collision. A collision map for suspension droplet collisions will be derived. The formation of satellite droplets by suspension droplets collisions is correlated by a function based on the basic parameters and dimensionless numbers of the process. The results support the understanding of the phenomena of binary droplet collision dynamics between droplets from pure fluids and suspensions.

### INTRODUCTION

The collision process of liquid drops is of common interest in several engineering process, especially within liquid spray systems as e.g. in spray drying [1]. Many numerical and experimental studies have been carried out on binary collisions of mostly equal sized droplets from pure fluids (water, fuels, alcohols,...).

A comprehensive review of droplet collision experiments on water and fuel drops has given by Orme [2]. A series of investigations as those of Brazier-Smith et al. [3], Arkhipov et al. [4], Ashgriz and Poo [5] and fuel drop collisions of Jiang et al. [6], Qian and Law [7] has been performed. For the characterization of the collision phenomena, these researchers used the Weber number, the impact parameter and the diameter ratio of the colliding droplets. For the outcome of collisions of hydrocarbon drops and water drops in a gas field, five phenomenological regions have been identified and summarized in collision charts. Comparing the collision outcomes of hydrocarbon drops and water drops it is estimated, that for the case of water drops typically no "bouncing" of droplets occurs and beside the region "stretching separation" and "reflexive separation" after collision the region of "coalescence" exists. The authors showed in their experimental work, that the difference in droplet collision outcomes of water and hydrocarbon is referred to the different liquid properties (viscosity and surface tension). Furthermore, by increasing the pressure and the density of ambient gas, the tendency of "bouncing" of droplets increases even within central collisions.

In binary collision experiments of ethanol drops [8] these results were verified for other Weber numbers. The phenomenon of binary collision of propanol drops for higher

Weber numbers ( $>1000$ ) has been experimentally investigated by Frohn and Brenn [9] and by Roth et al. [10] in comparison with results of numerical simulations. In some investigations with water drops the bouncing collision outcome where the two drops bounce without forming any ligament for low Weber numbers and high impact parameters was not noticed [11].

The influence of the liquid viscosity on the collision outcome has been investigated by Havelka et al. [11]. The collision outcome of water drops and Triethylenglycol drops is compared, where Triethylenglycol has a higher viscosity than water. In a region of Weber numbers up to 350 the results showed that for Triethylenglycol drops no region of "reflexive separation" exist. Only the collision outcomes "bouncing", "coalescence" and "stretching separation" has been detected. The transition from the region "coalescence" to "stretching separation" was detected at higher Weber numbers.

Blei and Sommerfeld [12, 13] investigated the collision event of emulsion droplets with identical concentration (process fluids: Soy based and whey based milk product), where „Soy“ exhibits a non-Newtonian behaviour and „Whey“ a Newtonian behaviour. The results have been compared with results of Havelka et al. [11]. It was shown that the collision outcome of the non-Newtonian liquid droplets is comparable with the impact outcome of Newtonian drops with identical liquid properties (viscosity, surface tension and density). It has been confirmed experimentally, that by increasing the liquid viscosity the transition limit between the region "coalescence" and the region "stretching separation" is shifted to higher Weber numbers.

Willis et al. [14] investigated binary droplet collisions under vacuum conditions in order to examine the role of the viscosity for colliding droplets. They have shown that compared to a collision under ambient pressure the influence of the viscosity for the collision process under vacuum is well pronounced. The critical Weber numbers (transition limits) is shifted to higher values.

Menchaca-Rocha et al. [15] studied the collision outcome of mercury drops, while slipping on a glass plate and showed that the impact effects are comparable to the collision effects of free falling liquid droplets.

Brenn and Kolobaric [16] investigated the formation of satellite droplets in the “stretching separation” region in unstable binary collisions of equal-sized drops for propanol-2 and acetone. Stability nomograms have been outlined to identify areas of constant satellite droplet numbers. A model for the process of satellite droplet formation has been proposed.

Gao et al. [17] studied the collision of drops of unlike liquids, the collision between a water drop and an ethanol drop. Due to the large difference in surface tension for water and ethanol, an “unbalanced surface force” action was observed on the water drop.

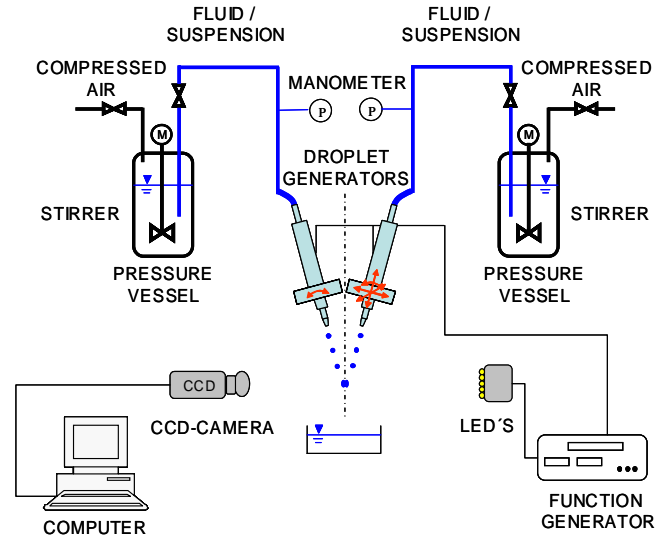
The application of these results for liquid droplet collisions for interpretation in other relevant technical processes dealing with difficult process fluids especially suspensions is limited. In this paper the results of droplet collision investigations using different suspension properties will be presented. The formation of satellite droplets for the case of the “stretching separation phenomenon” in binary collisions of equal sized droplets is the subject of particular interest.

## EXPERIMENTAL WORK

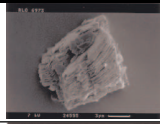

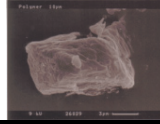
The laboratory spray rig is shown schematically in **Fig. 1**. The central devices of the set-up are two piezoelectric droplet generators. One drop generator is mounted on a three-dimensional traversing unit and the other drop generator is kept fixed. To vary the collision angle ( $\alpha$ ), the direction of the droplet streams of both droplet generators can be adjusted at different angles. In the present investigation the collision angle is constant as  $\alpha = 60^\circ$ . The feed to the droplet generators is carried out with separate pressure vessels that are equipped with stirring elements to prevent sedimentation of the particles. The liquid flow is forced through a nozzle by means of a pressure, where a jet with a defined velocity is generated. In order to produce droplets of equal size (monodisperse drops), the piezoceramic vibrator of the drop generator is excited by an appropriate electrical signal [18]. Two droplet streams in a diameter range of 370-380 $\mu\text{m}$  have been produced. The droplet velocities of the streams of liquid and suspension drops have been varied systematically to change the Weber number and impact parameter of the collision.

For visualization of the collision interactions of the drops, a CCD-camera is used in combination with a matrix of LED's for a transmitted light illumination of the droplet chain. The camera and illumination device are placed on a separate traverse unit to enable changes of the position without disturbing the drop streams. Only one function generator is used to drive the LED's, which is synchronized with the excitation signal for the drop generators. As a result,

the collision outcome may be recorded by the CCD-camera as fixed image.



**Fig. 1: Spray rig for analysis of collision interactions of the drops.**

Solid particle			
China Clay-I / China Clay-II		Diameter $d_{50,3}$ [ $\mu\text{m}$ ]	Density $\rho_p$ [ $\text{g}/\text{cm}^3$ ]
		10 / 2	2.6
Glass - Silibeads		4	2.5
Polyamid 12		7	1
Pure liquid			
Water		Water	
$(\rho = 1\text{g}/\text{cm}^3, \sigma = 72\text{mN}/\text{m}, \eta = 1\text{mPas})$			
50w.% Ethanol in Water		50w.% Ethanol in Water	
$(\rho = 0.913\text{g}/\text{cm}^3, \sigma = 27\text{mN}/\text{m}, \eta = 1.1\text{mPas})$			
Drop 1		Drop 2	
Water as carrier liquid (Influence of particle concentration)			
Suspension with China Clay-I $c_p$ [w.%]		Suspension with China Clay-I $c_p$ [w.%]	
0; 0.3; 0.5; 1; 5; 10; 15		0; 0.3; 0.5; 1; 5; 10; 15	
Drop 1		Drop 2	
Water and Water-Ethanol as carrier liquid (Influence of particle size)			
Suspension with $c_p = 10\text{w.}\%$		Suspension with $c_p = 10\text{w.}\%$	
Polyamid 12 ( $d_{50,3} = 7\mu\text{m}$ )		Polyamid 12 ( $d_{50,3} = 7\mu\text{m}$ )	
Glass ( $d_{50,3} = 4\mu\text{m}$ )		Glass ( $d_{50,3} = 4\mu\text{m}$ )	
China Clay-II ( $d_{50,3} = 2\mu\text{m}$ )		China Clay-II ( $d_{50,3} = 2\mu\text{m}$ )	

**Table 1: Pure liquids and process suspensions used in the experiments at room temperature.**

In order to determine the effect of the suspended solid particles on the collision interactions of the drops, different model suspensions based on water and water-ethanol-mixture with various suspended China Clay-I / -II, Glass and Polyamid particle concentrations were used. China Clay-I / -II and Glass particles were suspended in water and Polyamid particles in water-ethanol-mixture. For the suspensions under investigations no stabilizer has been added. These particles have spherical and non spherical shape (Table 1).

In order to be able to evaluate the effect of the carrier liquid by impact with solid particles on collisional interactions of the drops, experiments have been carried out under comparable conditions with and without particle loading. For the characterization of the collision conditions the Weber number and the impact parameter are used. The Weber number ( $We$ ) is defined as

$$We = \frac{\rho \cdot D \cdot u^2}{\sigma}, \quad (1)$$

where  $\rho$  is the density,  $\sigma$  the surface tension,  $D$  the diameter of the liquid drop and  $u$  the relative velocity of the two drops. In the case of pure liquid the liquid density is used to define the Weber number. For the suspension drops, the density of the density mixture, dependent on the concentration of particles is utilized. The relative velocity is calculated as

$$u = (u_1^2 + u_2^2 - 2u_1 u_2 \cos \alpha)^{1/2}, \quad (2)$$

where  $u_1$  is the velocity of drop1,  $u_2$  the velocity of drop2 and  $\alpha$  is the collision angle [19].

Second important parameter is the impact parameter ( $B$ ), which characterizes the geometry of impact:

$$B = \frac{\chi}{r_1 + r_2} = \sin \psi. \quad (3)$$

The impact parameter represents the position of the droplets  $\chi$  at the moment of contact perpendicular to the direction of their relative velocity.

By considering the head-on collision of two equal size droplets the relative velocity vector coincides with the centre-to-centre line (i.e.  $B = 0$ ). An increase in the impact parameter will lead to an off-centre collision (i.e.  $B > 0$ ) until the droplets do not collide each other (i.e.  $B = 1$ ) [19].

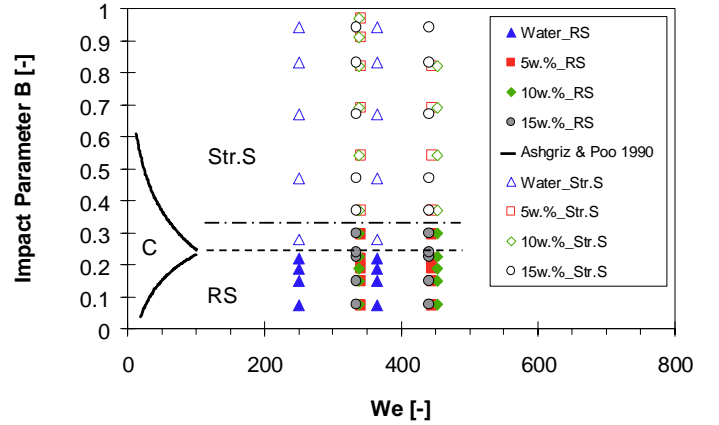
The Weber number was mainly controlled by changing the relative velocity, which was adjusted by the mass flow rate. The impact parameter was varied by positioning the movable drop generator relative to the fixed one in the normal direction to the plane of view of Fig. 1.

The visualization system was used to record the collision outcome as fixed image. The results were obtained by evaluation of the records. All experiments have been carried out multiple times to be sure that the collision conditions are reproducible. For a clear representation of experimental results only average data in terms of secondary droplet number has been discussed in this paper. The scatter of the measured data is small.

## RESULTS

### Collision regimes of binary collision of droplets with and without particle loading

The phenomena of binary collision of water and suspension droplets of equal size in the Weber-number range  $We > 100$  is experimentally investigated. Suspensions based on water with different suspended China Clay-I particle concentrations are used here. The derived collision regime map is shown in Fig. 2.



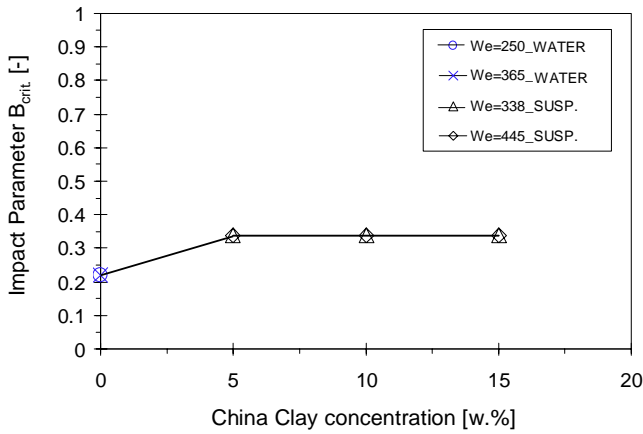
**Fig. 2: Collision regime map of suspension droplets with different particle loadings (China Clay-I) and water droplets under ambient pressure.**

In the studies of Ashgriz and Poo [5] for water droplets under ambient pressure three regions for different types of collision outcomes have been identified. Comparison of collision outcomes of water droplets in the Weber number range up to  $We = 100$  the results show, that in addition to the region reflexive separation (“RS”) and stretching separation (“Str.S”) a region coalescence (“C”) exists. Moreover for water it was observed that with increasing Weber number the coalescence region becomes narrower and the reflexive separation and stretching separation regions are possibly overlapped. The boundary of the different regions in the diagram is identified by a continuous line. The results of binary droplet collisions of suspensions with identical particle loading of 5, 10 and 15w.% and water for varied Weber numbers are included in Fig. 2. For  $250 < We < 450$  it can be seen, that both, suspension droplets and water droplets, have no region of coalescence. For these Weber-number range solely two collision outcomes, namely reflexive separation (“RS”) and stretching separation (“Str.S”) are identified. The transition limit between “RS” and “Str.S” for the case of water droplet collisions is shown by the dashed line. For the case of suspension droplets this transition limit is shifted to higher impact parameters (dashed-dotted line). It can be seen, that with the addition of solid particles in the carrier liquid (particle concentration of 5 to 15w.%) the determined critical value of the impact parameters is constant. The influence of the particle concentration in droplets on the collision outcome is not observable.

This trend is illustrated in Fig. 3 for the critical value of the impact parameter depending on particle concentration for the Weber-number range in question.

In the following, the formation of satellite droplets for the case of the “stretching separation phenomenon” (impact parameter of  $B > 0$ ) in binary collisions of equal sized

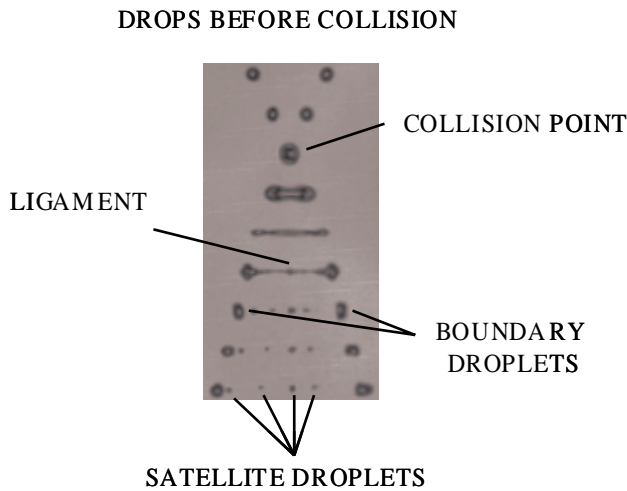
droplets is of particular interest. These studies are of importance in industrial applications as spray drying in order to analyze the formation of fine particles (dust) [1].



**Fig. 3: Critical value of impact parameters versus particle loading (China Clay-I) for different Weber numbers.**

#### Binary collision of suspension droplets

Figure 4 illustrates droplet impacts of equal sized water droplets for the case of the “stretching separation phenomenon”. A ligament formation process is to be seen starting at the collision point, which finally results in the formation of satellite droplets when the connecting neck is pinched off [7]. The satellite droplets diameter is much smaller than the initial droplets diameter. The analysis of the amount of satellite droplets was performed by means of an image processing tool.

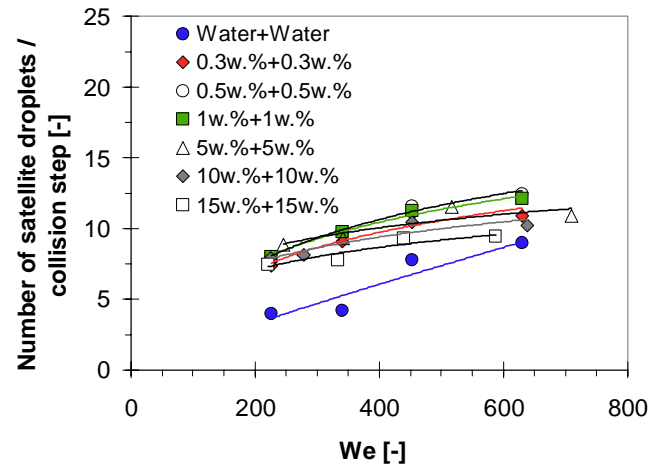


**Fig. 4: Droplet impacts of equal sized water droplets for the case of the “stretching separation phenomenon”.**

When adding solid particles to the water the colliding phenomena shows an unstable formation of satellite droplets to the colliding case with pure water. This formation behaviour becomes more pronounced by increasing the particle concentration from 5w.% up to a particle concentration  $c_p = 15w.%$ . As can be seen from Fig. 4 for pure water for one collision process the size of the satellite droplets is not equal, however, the size distribution is equal

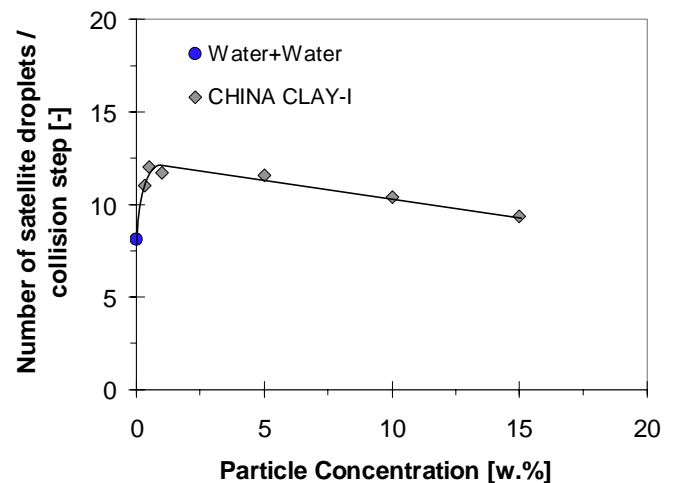
for each collision process. These changes by adding solid particles to the carrier liquid water, which have a random distribution in the ligament formed during the collision and influence obviously the collision process [19].

The resulting number of satellite droplets for impact parameter  $B = 0.83$  and different Weber numbers are shown in Figure 5. The number of satellite droplets for the six cases ( $c_p = 0.3, 0.5, 1, 5, 10$  and  $15w.%$ ) have a minimum for low Weber numbers and increases by increasing the Weber number from  $We \sim 300$  to  $We \sim 450$ . For  $c_p = 0.5w.%$  the measured number of satellite droplets is larger than for  $c_p = 1w.%, 5w.%$  and  $10w.%$ , and at the highest particle loading  $c_p = 15w.%$ , the lowest satellite droplet number is counted. By decreasing the particle concentration ( $c_p = 0.3w.%$ ) the satellite droplets number for suspensions decrease again to a value of the pure water.



**Fig. 5: Number of satellite droplets versus We number for different particle (China Clay-I) loadings of two suspension drops at  $B = 0.83$ .**

This trend is illustrated in Figure 6 for the number of satellite droplets depending on particle concentration at  $We = 500$  and an impact parameter  $B = 0.83$ .



**Fig. 6: Number of satellite droplets versus particle concentration for China Clay-I at  $We = 500$  and an impact parameter  $B = 0.83$  for identical particle size  $d_{50,3} = 10\mu m$ .**

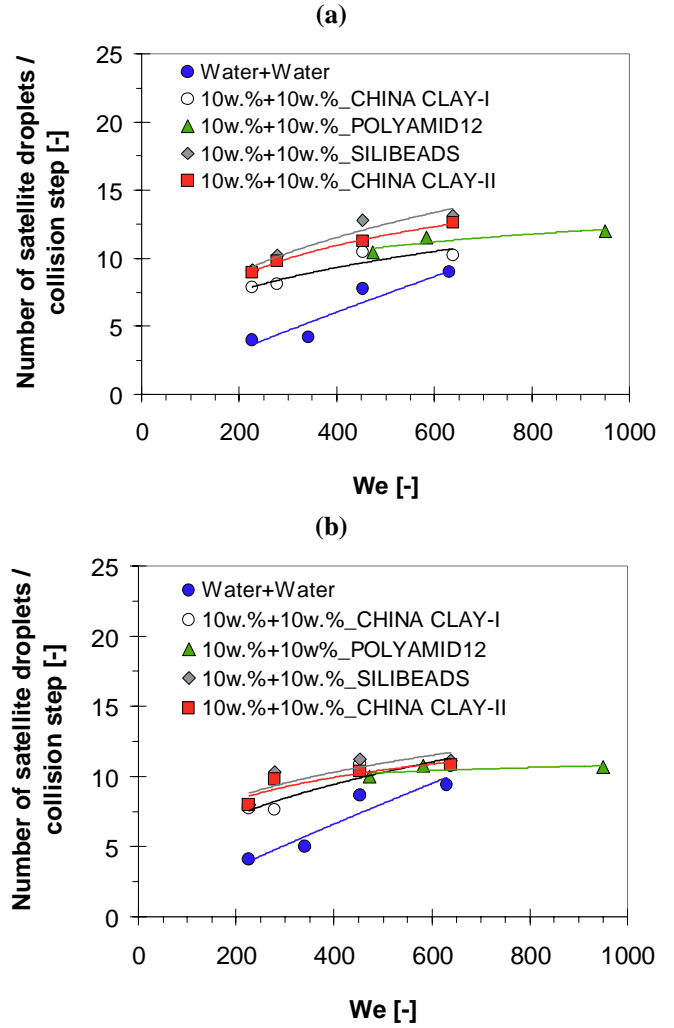
The formation of satellite droplets is influenced by the particle loading of the carrier liquid. By increasing the

particle concentration the satellite droplet number values decreases due to the decreased length of the ligament at break-up. A higher concentration of particles stimulates the perturbations developed after the collision, and spatial and temporal break-up of the ligament becomes faster. As a result, the number of satellite droplets decreases. By increasing the impact parameter from  $B = 0.83$  to  $B = 0.92$  the same trend of the satellite droplet number is noticed. An influence of the impact parameter of the satellite droplet number in this case is not observable. The limiting behaviour for increasing Weber numbers may be referred to the particle size, when the diameter of the ligament at break-up is in the order of the particle size.

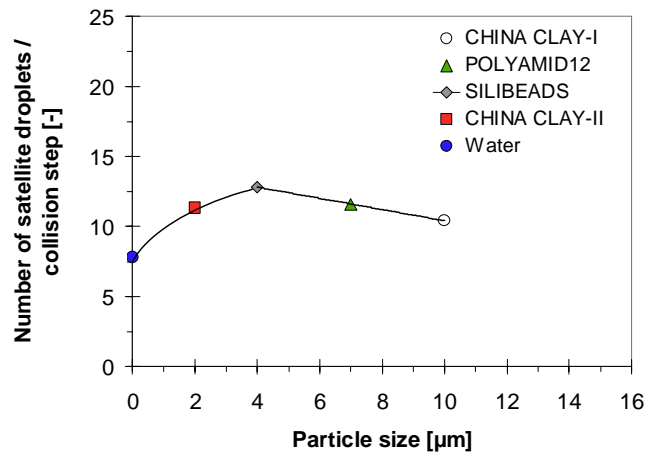
For suspension droplets with particle loading  $c_p = 5w. \%$  (which has an average number of China Clay-I particles per volume of  $36765 / \text{mm}^3$  using  $d_{50,3} = 10\mu\text{m}$  for calculation), the ligament length and thickness at break-up has been detected. The thickness of the ligament at break-up decreases with increasing the Weber number while the length of the ligament at break-up is increasing [19]. From this behaviour it can be concluded that at lower Weber numbers ( $We \sim 200$ ) the solid particles are still good covered in the ligament at break-up. At higher Weber numbers ( $We$  up to  $\sim 500$ ) the solid particle sizes are in the order of the diameter of the ligament at break-up ( $30 - 40\mu\text{m}$ ). That means, with increasing Weber number a critical value is reached where the number of satellite droplets becomes constant.

**Fig. 7a-b** illustrates the resulting number of satellite droplets for the collision of suspension droplets with identical particle loading  $c_p = 10w. \%$  when using different particles for an impact parameter of  $B = 0.83$  and  $B = 0.92$ . The influence of the particle size on the satellite droplet formation is seen in Fig. 7a. The satellite drop numbers for the investigated cases (China Clay-I –  $d_{50,3} = 10\mu\text{m}$ , Polyamid –  $d_{50,3} = 7\mu\text{m}$ , Silibeats –  $d_{50,3} = 4\mu\text{m}$ , China Clay-II –  $d_{50,3} = 2\mu\text{m}$  and water) have similar tendencies. The numbers of satellite droplets have a minimum for small Weber numbers and increase by increasing the Weber number to a maximum. Comparing the results for the collision process for suspension droplets with different particle size among each other, it is shown that the formation of satellite droplets is influenced by the particle size. By increasing the particle size the satellite droplet number decreases. At an impact parameter  $B = 0.92$  (Fig. 7b) a similar trend of the satellite droplet number is noticed, but the saturation behaviour starts at smaller Weber numbers.

The number of satellite droplets versus the solid particle size within the suspension at an impact parameter  $B = 0.83$  and at a Weber number  $We = 500$  is shown in **Fig. 8**. The number of satellite droplets decreases with increasing particle sizes. The decrease of the satellite droplet number with increasing particle size is due to the relative particle size with respect to the length, respectively the ligament diameter at break-up. However, when using pure water without particle loading, one achieves another limit which may hold for an infinitely small particle size. In this case the smallest number of satellite droplets should be observed. By decreasing the particle size ( $d_{50,3} < 4\mu\text{m}$ ) the satellite droplets number for suspensions decreases again to a value of the pure liquid. Here the suspension viscosity effect, considering the suspension with smaller particles as a colloidal system, may contribute. Further investigations with smaller particles (below  $2\mu\text{m}$ ) are needed in this area.



**Fig. 7: Number of satellite droplets versus We number for different particle types and sizes of two suspension drops at (a)  $B = 0.83$  and (b)  $B = 0.92$ .**



**Fig. 8: Number of satellite droplets versus particle size for different particle types with identical particle loading  $c_p = 10w. \%$  of two suspension drops at  $We = 500$  and  $B = 0.83$ .**

The number of secondary droplets for China Clay-I at an impact parameter  $B = 0.83$  can be correlated by

$$N_{Sec.} = We^{0.264} \cdot Re^{0.042} \cdot \omega^{-0.133} \quad (4)$$

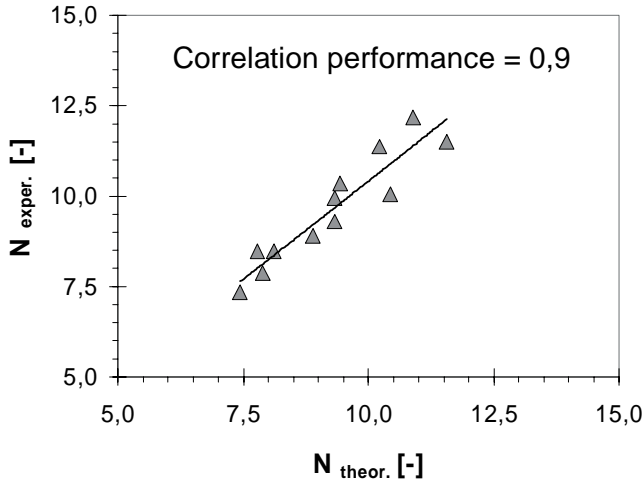
with a correlation performance of 0.9 (Fig. 9). For the correlation of the number of secondary droplets the Reynolds number (Re) and the particle loading ( $\omega$ ) are used in addition to the Weber number. The Reynolds number is defined as

$$Re = \frac{\rho \cdot D \cdot u}{\eta}, \quad (5)$$

where  $\rho$  is the density,  $\eta$  the dynamic viscosity, D the diameter of the liquid drop and u the relative velocity of the drop. The loading of solid particles is defined as

$$\omega = \frac{M_{Solid}}{M_{Liquid}}, \quad (6)$$

where  $M_{Solid}$  is the mass of solid and  $M_{Liquid}$  is the mass of a droplet.



**Fig. 9: Correlation of number of secondary droplets for China Clay-I at an impact parameter  $B = 0.83$  for different particle loading ( $c_p = 5, 10$  and  $15w.\%$ ).**

## SUMMARY AND CONCLUSIONS

An experimental study of binary collisions of suspension drops in off-center collisions has been carried out. The formation of satellite droplets by stretching separation phenomenon in binary collisions of drops of liquids with and without particle loading has been investigated. In order to determine the effect of suspended solid particles concentration and size on the collisional interactions of the drops, process suspensions based on water and water-ethanol-mixture with various suspended China Clay, Silibeads and Polyamid particle concentrations were used.

The phenomena of binary collision of water and suspension droplets of equal size in the Weber-number range  $We > 100$  is experimentally investigated. Suspensions based on water with different suspended China Clay-I particle

concentrations are used here. For the Weber-number range  $250 < We < 450$  solely two collision outcomes, namely reflexive separation (“RS”) and stretching separation (“Str.S”) are identified. No region of coalescence is observable. For the case of suspension droplets the transition limit between “RS” and “Str.S” is shifted to higher impact parameters than for the case of water droplet collisions.

Measurements of the number of satellite droplets with different particle (China Clay-I loadings have shown that the increase of the solid particle concentration leads to a decrease in the satellite droplet number. Here the influence of the solid particle concentration is more significant than that of the viscosity. Furthermore due to cover performance of solid particles in the ligament at break-up, it can be concluded that with increasing Weber number a critical value is reached where the number of satellite droplets becomes constant (saturation behaviour). This saturation behaviour could also be the case for water for higher Weber numbers, which is not considered in our examinations.

The results for the collision process for suspension droplets with different particle type and size show, that the formation of satellite droplets is also influenced by the particle size. By increasing the particle size the satellite droplet number decreases.

## ACKNOWLEDGMENT

The authors gratefully acknowledge the financial support for this project SCHU 472/13-2 by the German Research Foundation (Deutsche Forschungsgemeinschaft, DFG).

## NOMENCLATURE

Symbol	Quantity	SI Unit
B	Impact parameter (geometry of impact)	$m^2$
$c_p$	Particle concentration	
$d_{50,3}$	Median diameter of solid particles	
D	Diameter of droplet	
$M_{Liquid}$	Mass of liquid	
$M_{Solid}$	Mass of solid	
$N_{Sec.}$	Number of secondary droplets	
$r_1$	Radius of drop1	
$r_2$	Radius of drop2	
Re	Reynolds number ( $= \rho \cdot D \cdot u / \eta$ )	
u	Relative velocity of the two drops	
$u_1$	Velocity of drop1	
$u_2$	Velocity of drop2	
We	Weber number ( $\rho \cdot D \cdot u^2 / \sigma$ )	
$\alpha$	Collision angle	
$\chi$	Position of the droplets at the moment of contact	
$\eta$	Viscosity of droplet	
$\rho$	Density of droplet	
$\sigma$	Surface tension of droplet	
$\omega$	Nondimensional particle loading ( $= M_{Solid} / M_{Liquid}$ )	

C	Coalescence
RS	Reflexive separation
Str.S	Stretching separation
Susp.	Suspension

## REFERENCES

- [1] R.E.M. Verdurmen, P. Menn, J. Ritzert, S. Blei, G.C.S. Nhumaio, T. Sonne Sørensen, M. Gusing, J. Straatsma, M. Verschueren, M. Sibeijn, G. Schulte, U. Fritsching, U., K. Bauckhage, C. Tropea, M. Sommerfeld, A.P. Watkins, A.J. Yule and H. Schönfeldt, Simulation of agglomeration in spray drying installations: the EDECAD project, *Drying Technol.* 22, pp. 1403-1461, 2004.
- [2] M. Orme, Experiments on droplet collisions, bounce, coalescence and disruption, *Prog. Energy Combust. Sci.*, vol. 23, pp. 65-79, 1997.
- [3] P.R. Brazier-Smith, S.G. Jennings and J. Latham, The interaction of falling water droplets: Coalescence, *Proc. R. Soc. Lond. A*, vol. 326, pp. 393-408, 1972.
- [4] V. Arkhipov, G. Ratanov and V. Trofimov, Experimental study of droplets interaction at collisions, *J. Appl. Mech. Tech. Phys.* 2, pp. 73-77, 1978.
- [5] N. Ashgriz and J.Y. Poo, Coalescence and separation in binary collisions of liquid drops, *J. Fluid Mech.*, vol. 221, pp. 183-204, 1990.
- [6] Y.J. Jiang, A. Umemura and C. K. LAW, An Experimental Investigation on the collision behaviour of hydrocarbon droplets, *J. Fluid Mech.*, vol. 234, pp. 171-190, 1992.
- [7] J. Qian and C.K. Law, Regimes of coalescence and separation in droplet collision, *J. Fluid Mech.*, vol. 331, pp. 59-80, 1997.
- [8] J.-P. Estrade, H. Carentz, G. Lavergne and Y. Biscos, Experimental investigation of dynamic binary collision of Ethanol Droplet-Model for droplet coalescence and bouncing, *Proc. ILASS '98 Manchester*, pp. 528-533, 1998.
- [9] A. Frohn and G. Brenn, Collision and merging of two equal droplets of propanol, *Experiments in Fluids*, vol. 7, pp. 441-446, 1989.
- [10] N. Roth, M. Rier and A. Frohn: High energy head-on collision of droplets, *Proc. ILASS-Europe'99*, pp. 1-5, 1999.
- [11] P. Havelka, C. Gotass, H. Jakobsen and H. Svendsen, Droplet formation and interactions under normal and high pressure, *Proc. ICMF 2004, Yokohama/Japan*, Paper No. 123, 2004.
- [12] S. Blei and M. Sommerfeld, Experimentelle Untersuchung von Tropfenkollisionen als Basis Lagrangscher Modellierungen, *Proc. Spray 2002, Freiberg/Deutschland*, pp. 295-304, 2002.
- [13] S. Blei and M. Sommerfeld, Investigation of droplet collisions of viscous process fluids by imaging techniques, *ILASS 2004, Nottingham/England*, pp. 100-105, 2004.
- [14] K. Willis and M. Orme, Binary droplet collisions in a vacuum environment: An Experimental Investigation of the role of viscosity, *Experiment in Fluids*, vol. 34, pp. 28-41, 2003.
- [15] A. Menchaca-Rocha, F. Huidobro, A. Martinez-Davalos, K. Michaelian, A. Perez and V. Rodriguez, Coalescence and fragmentation of colliding mercury drops, *J. Fluid Mech.*, vol. 346, pp. 291-318, 1997.
- [16] G. Brenn and V. Kolobaric, Satellite droplet formation by unstable binary drop collisions, *Physics of Fluids*, vol. 18, pp. 1-18, 2006.
- [17] T.-C. Gao, R.-H. Chen, J.-Y. Pu and T.-H., Lin, Collision between an ethanol drop and a water drop, *Experiments in Fluids*, vol. 38, pp. 731-738, 2005.
- [18] H. Ulmke, T. Wriedt and K. Bauckhage, Piezoelectric Droplet Generator for the Calibration of Particle-Sizing Instruments, *Chem. Eng. Technol.*, vol. 24, No. 3, pp. 265-268, 2001.
- [19] O. Kurt, U. Fritsching and G. Schulte, Binary Collisions of Droplets with Fluid and Suspension Particles, *ILASS 2007, Mugla, Turkey*, 10-12 September, 2007.
- [20] O. Kurt, U. Fritsching and G. Schulte, Secondary Droplet Formation During Binary Suspension Droplet Collisions, accepted in: *Atomization and Sprays*, April 2008.